Original Article: Degradation of Methyl Orange Under Visible Light by ZnO-Polyaniline Nanocomposites

RajeshJ.Kavade[a] |Renukacharya Ganpati Khanapure[a] | U. S. Gavali[a]|A.A. Patil[b]|Suresh Vasant Patil[a,*]

[a]Karmaveer Bhaurao Patil Mahavidyalaya Pandharpur (Autonomous) Dist Solapur.PIN 413304 M.S. India
[b]K.N.Bhise Arts, Commerce and Vinaykrao Patil Science College, Kurduwadi, Dist.Solapur. M.S. India

Use your device to scan and read the article online

Citation R.J. Kavade, R.G. Khanapure, U.S. Gavali, A.A. Patil, S.V. Patil*. **Degradation of Methyl Orange Under Visible Light by ZnO-Polyaniline Nanocomposites**. *J. Appl. Organomet. Chem.*, **2022**, *2*(2), 89-100.

https://doi.org/10.22034/jaoc.2022.349558.1056

Article info:
Received: 2022-06-29
Accepted: 2022-07-31
Available Online: 2022-08-08
ID: JAOC-2206-1056
Checked for Plagiarism: Yes
Peer Reviewers Approved by:
Dr. SUNIL V. GAIKWAD
Editor who Approved Publication:
Professor Dr. AbdelkaderZarrouk

Keywords:
Photodegradation, ZnO-Polyaniline nanocomposite, Methyl orange, Visible light, Room temperature, XRD, SEM.

ABSTRACT

The ZnO-Polyaniline nanocomposites with 9:1, 8:2, and 7:2 ratios were successfully synthesized by using a grinding method in ethyl alcohol. The XRD, TEM, and SEM characterizations are used for nanocomposites analysis. The entire three nanocomposites were degraded by methyl orange in the presence of visible light. We get the best results for ZnO-Polyaniline (7:3) catalyst. About 82% degradation of methyl orange was observed below visible light within 140 minutes.

Introduction

Nowadays, the increasing population has mostly contributed to a rise in groundwater and surface water pollution. Since they cannot biodegrade, are extremely poisonous to aquatic life, and have a carcinogenic effect on people, organic dyes used in the fabric, and food stuff productions are significant causes of environmental pollution. Methyl orange is a highly toxic chemical that is mainly applicable for as a dye [1-4]. In directive to decrease organic dye pollution to the humans and environment, photo catalysts have remained studied extensively for their ability to break down

Corresponding Author:Suresh Vasant Patil (sureshpatil1385@gmail.com)

organic mixtures in polluted air, or aquatic, or to transfer them to harmLess chemicals. The metal oxide nanoparticles like ZnO [5] and TiO_2 [6-9] have remained extensively used to destroy non-biodegradable dyes by photo catalytic ways, so the investigators to cause to growing degradation proportion of contaminants by doping inorganic solid through conductive polymers to realize synergetic and complementary behaviors between the polymer and inorganic material [10-19]. The term "good holes conducting materials" refers to a variety of conducting polymers [14-15]. These conducting polymers act as surface stabilizers or coping agents when coupled with metals or semiconducting nanoparticles [16–19]. ZnO has a decreased emission because of its extensive band gap semiconductor (3.37 ev) and 60 MeV excitation binding energy at room temperature [20]. The huge band gap of ZnO makes it a suitable material for collecting energy photons (UV radiation) [21]. The absorbed radiation acts as thermal energy in the photo catalytic reaction and stimulates the electrons from the valence band to the conduction band. Therefore, one of the most crucial characteristics that significantly affect biological conversions is band gap width. Because a wider band gap requires more energy to excite the electrons, only radiation with a higher energy, such as microwave and ultraviolet light, may be employed as the energy source of the reaction. Only catalysts with a narrow band gap can be driven by a lower energy visible light. These characteristics make it suitable for a series of optical and electrical uses such as photovoltaics, batteries, etc. [22–25].

Because of high conductivity, straightforward production process, and good environmental stability, numerous applications of polymers in catalysis are solid polymeric support, weakly cross-linked polymer, and non-crosslinked polymer fixed on solid support [26–28], Polyaniline (PANI) is a more promising polymer. Many inorganic acids, including phosphoric acid and sulfuric acid, are used in their production. However, the majority of PANI is created with weak HCl. The three main subtypes of polyaniline are pernigraniline, emeraldine, and leuco-emeraldine [29]. While polyaniline may be made from inorganic acids, it has some disadvantages such as making the compound intractable, difficult to work with, and infusible, all of which affect the conductivity of the substance. As a result, organic acids are utilized. PANI and its derivatives are regarded as one of the most competent classes of organic conducting polymers because of their well-behaved chemistry, simple protonation changeability, spectacular chemical reaction durability, and high environmental stability [30]. However, they are infrequently utilized for an extensive variety of applications, including light-emitting diodes, corrosion-resistant coatings, and electrostatic discharge protection [20–33]. Numerous studies have examined how adding polyaniline conducting polymers to ZnO nanostructures increases the UV emission and photocatalytic activity [7, 34].

The purpose of this work was to compare the photocatalytic movement of polyaniline homopolymer and ZnO-PANI composite for the methyl orange degradation under Ultra-violet and normal sunlight radiation. In the current study, the chemical oxidation of aniline was used for the first time to synthesize a PANI homopolymer and ZnO-PANI nanocomposite in an aqueous media. The PANI homopolymer was synthesized and the degradation of methyl orange (MO) dyes was monitored under the exposure to the natural sunlight and UV light. SEM and X-ray diffraction (XRD) were used to characterize the surface construction and morphology of the polyaniline homopolymer and ZnO-PANI nanocomposite. The remaining effects to be investigated were the effects of the

kind of organic dyes, light source, exposure period, photocatalyst quantity, and photocatalyst reuse on the photocatalytic movement.

Synthesis of nanocomposites

For the manufacture of zinc oxide nanoparticles, 50 mL of 0.5 N zinc acetate was added to 20 mL of 2% polyvinyl alcohol in a 500 mL beaker. For five minutes, the solution was swirled on a magnetic stirrer. When a white-colored precipitate of Zn $(OH)_2$ developed, 150 mL of 0.1 N NaOH solution was added by using a burette. The item was dried thoroughly after being filtered via Whatman filter paper number 41. To achieve a consistent particle size, the dry product was ground in 99.99 percent ethyl alcohol. To obtain the zinc oxide (ZnO), the ethyl alcohol was evaporated, and the finished product was heated to 3000 °C in a muffle furnace for four hours.

Synthesis of polyaniline

By polymerizing aniline with ammonium persulfate acting as an oxidant and hydrochloric acid serving as a catalyst, polyaniline was synthesized in 250 mL RB flask with a magnetic stirrer, 100 mL 1M HCl, and 4.8 mL of aniline. By using an ice and salt combination, the temperature was lowered to 0 °C. The above-mentioned solution was then gently mixed with 12 gm of an ammonium per sulfate solution in 30 mL of water. After that, the reaction was completed by stirring the mixture for 24 hours at 0 °C. Next, Whatman Paper No. 41 was used to filter the precipitate that had been produced. The product was thoroughly cleaned with distilled water until the solution was colorless. To eliminate chloride from the product, it was once again rinsed with distilled water.

Synthesis of ZnO-Polyaniline nanocomposites

The ZnO-Polyaniline nanocomposites were prepared by the physical grinding method. Three different composites were prepared (0.9 gm ZnO + 0.1 gm PANI, 0.8 gm ZnO + 0.2 gm PANI, and 0.7 gm ZnO + 0.3 gm PANI). These concentrations were taken in the different mortar and pestles with the addition of 10 mL of ethyl alcohol (99.99%), and then they were ground by hand to get a uniform and a well-distributed particle size. After getting the uniformLy colored nanocomposites, ethyl alcohol was evaporated to room temperature to get a fine powder of ZnO-Polyaniline nanocomposites.

Degradation of methyl orange

Preparation of solution: 0.75 gm of methyl orange (MO) was taken in a 100 mL beaker. After the preparing a clear-colored solution of methyl orange, the UV-Visible spectra were taken in the spectrophotometer. Then, 100 mg of ZnO-polyaniline catalyst (9:1 proportion) was added to the methyl orange solution, and the beaker was placed in a photoreactor with a constant stirring. A small quantity of methyl orange solution was taken in the cuvette and UV-Visible spectra were taken to examine the degradation of the sample. The concentration of Methyl orange dye was investigated by using the UV-Visible spectroscopy technique and the absorption of dye (MO) was quantified at a typical wavelength. The concentration of dye was calculated by standardization curves. In addition, the same procedure was followed for another two nanocomposites.

Results and Discussion

The XRD was used to analyze as-prepared ZnO nanoparticles, ZnO-Polyaniline nanocomposites, and polyaniline. The JCPD data (JCPDF No. 36-1451) of pure ZnO nanoparticles are compared with the XRD pattern. The entire peaks are similar to those of

the hexagonal phase with a wurtzite structure (Andlmar et. al., 2005). The diffraction peaks were observed for reflections from the planes [1 0 0], [0 0 2], [1 0 1], [1 0 2], [1 1 0], [1 0 3], [1 1 0], [1 1 0], [1 1 0], [1 1 0], [1 1 0], and [1 1 2] at the scattering angles 2 values of 31.52^0, 34.59^0, 36.03^0, 47.94^0, 56.75^0, 62.93^0, and 67.64^0. The pure ZnO's crystallinity was clearly seen in the XRD pattern. As seen in Figures 2-4, the crystallinity of the material declines and the distinctive height peaks of pure ZnO decrease steadily with a drop in particle size, increasing the amorphous nature of nanocomposites. Figures 1-5 display the XRD outlines of pure ZnO, PANI, and ZnO-PANI nanocomposite materials. As the proportion of polyaniline grows, two peaks can be observed in the pattern of pure ZnO. The greatest peak is about 18.5°, and it is attributed to the periodicity parallel and perpendicular to the PANI chain. Additionally, the peak at 20^0 shows the distinctive separation among the ring planes of the benzene rings in nearby chains or the tight contact. The number of peaks may also be attributed to the scattering from PANI chains at inter-planar spacing and reveals that the PANI also had some degree of crystallinity. The XRD pattern of ZnO-PANI nanocomposite exhibits peaks with the related PANI and recognizable ZnO nanoparticle peaks. Scanning electron microscopy (SEM) may be used to analyze the surface morphology of nanocomposites. The surface morphology of ZnO, ZnO-polyaniline nanocomposites, and pure polyaniline are shown in Figures 6–10. The grains were nodular, spherical, and had a homogenous distribution, with the majority of the grains being connected to one another, as could be observed from the photographs. When polyaniline concentration in pure ZnO increases, particle size decreases.

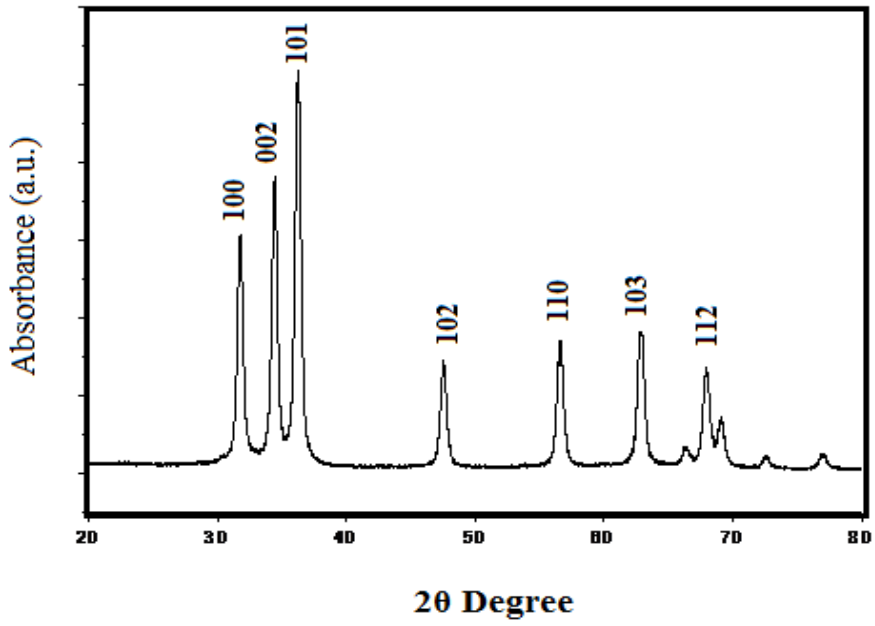

Figure 1. XRD pattern of pure ZnO nanoparticles

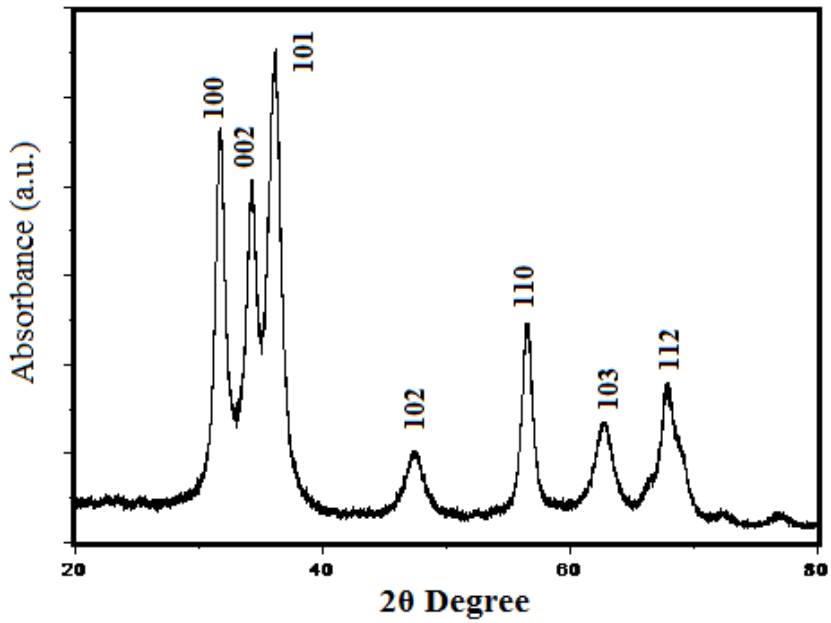

Figure 2. XRD pattern of $ZnO_{0.9}$-Polyaniline $_{0.1}$ nanocomposites

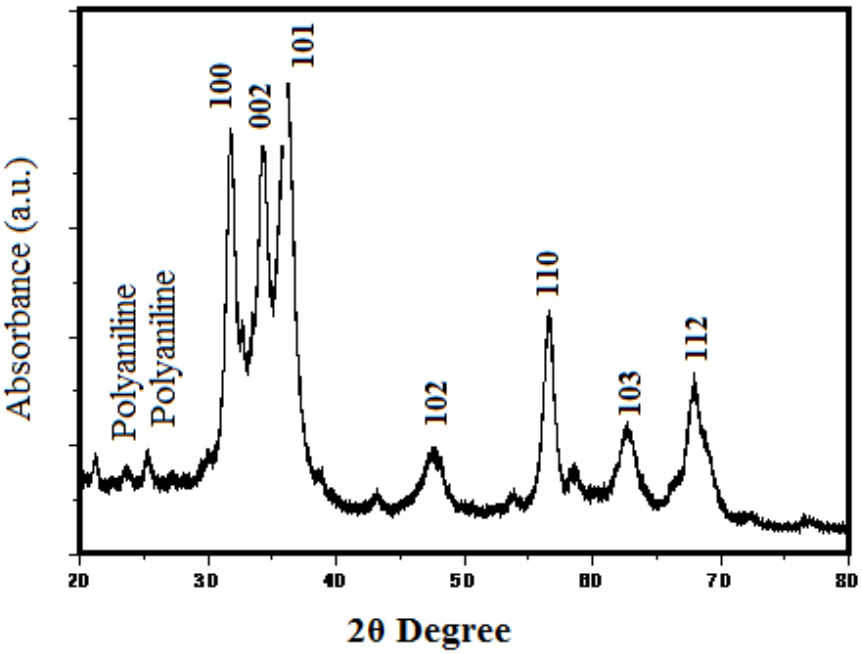

Figure 3. XRD pattern of $ZnO_{0.8}$-Polyaniline $_{0.2}$ nanocomposites

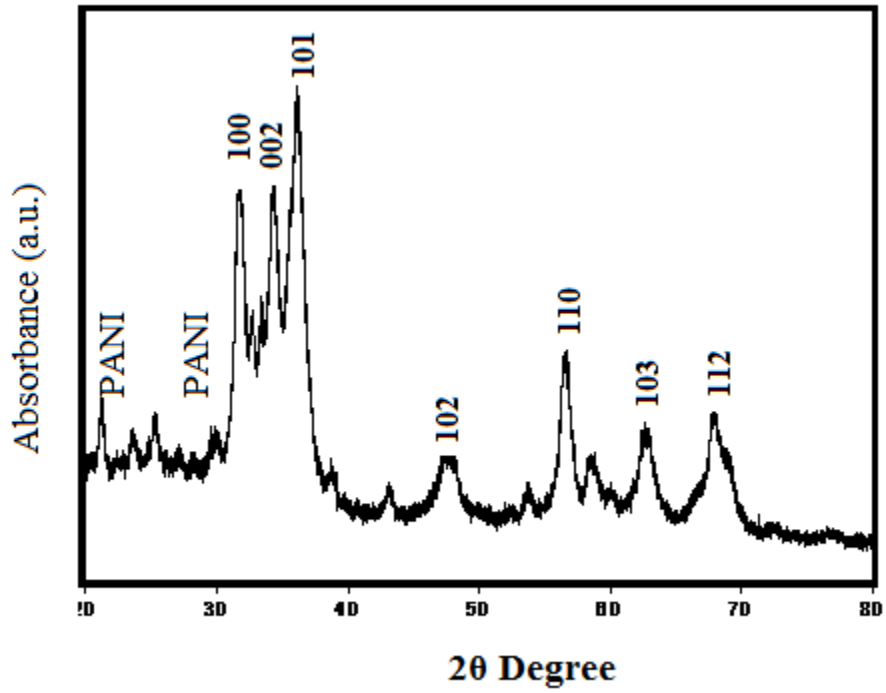

Figure 4. XRD pattern of $ZnO_{0.7}$-Polyaniline $_{0.3}$ nanocomposites

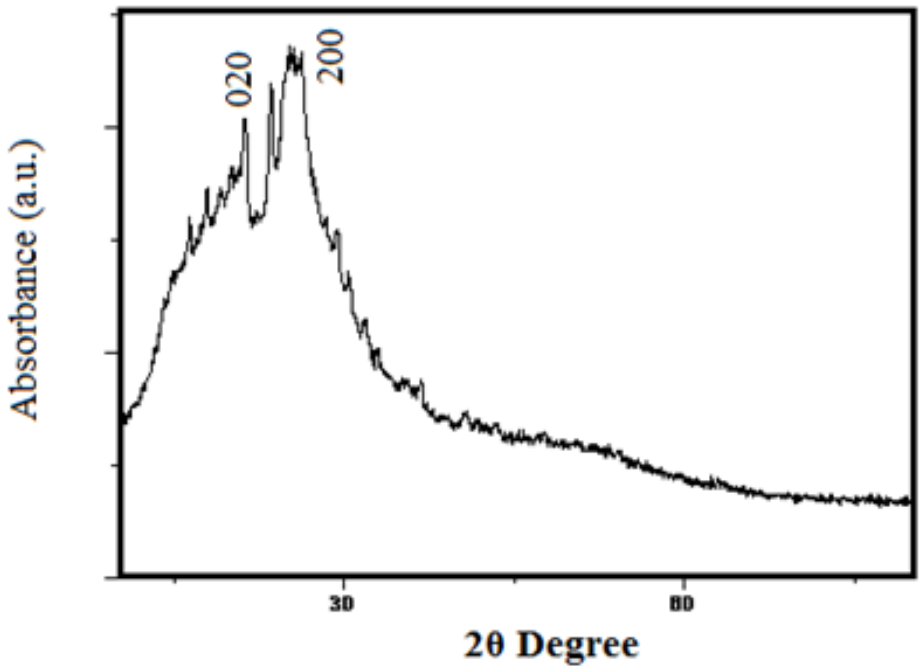

Figure 5. XRD of pure Polyaniline

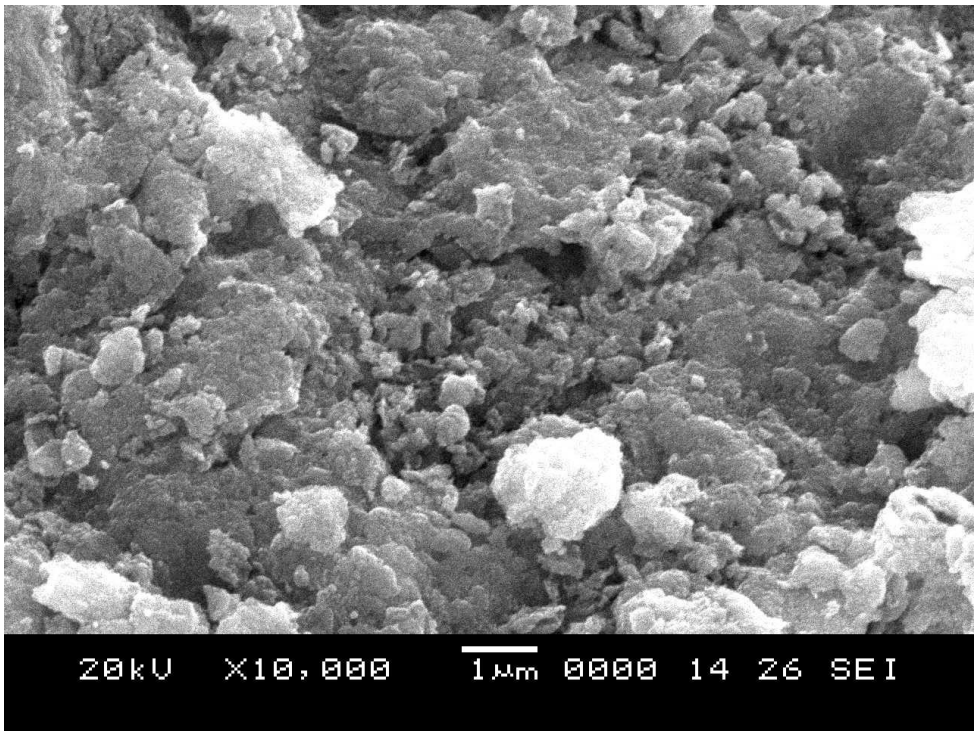

Figure 6. SEM of pure ZnO nanoparticles

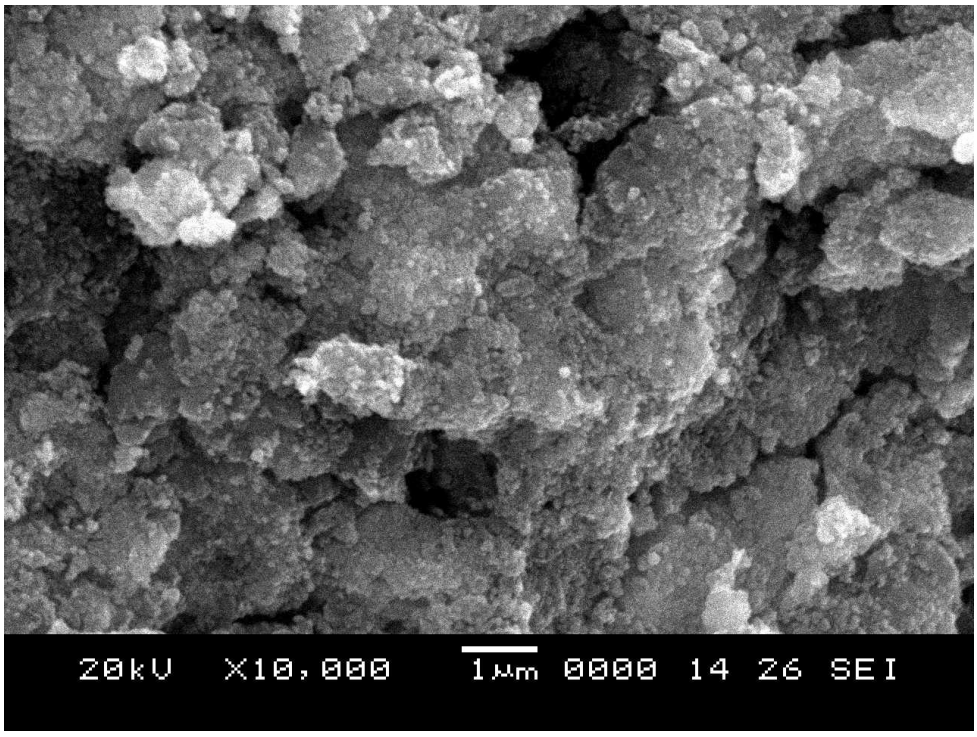

Figure 7. SEM of $ZnO_{0.9}$-Polyaniline $_{0.1}$ nanocomposites

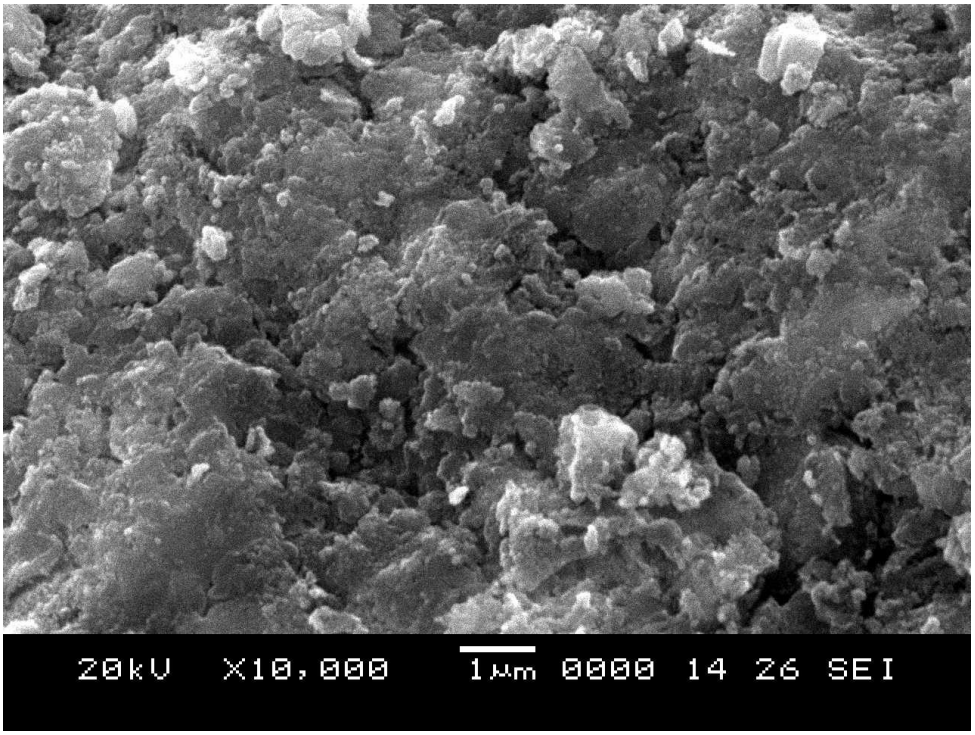

Figure 8. SEM of $ZnO_{0.8}$-Polyaniline $_{0.2}$ nanocomposites

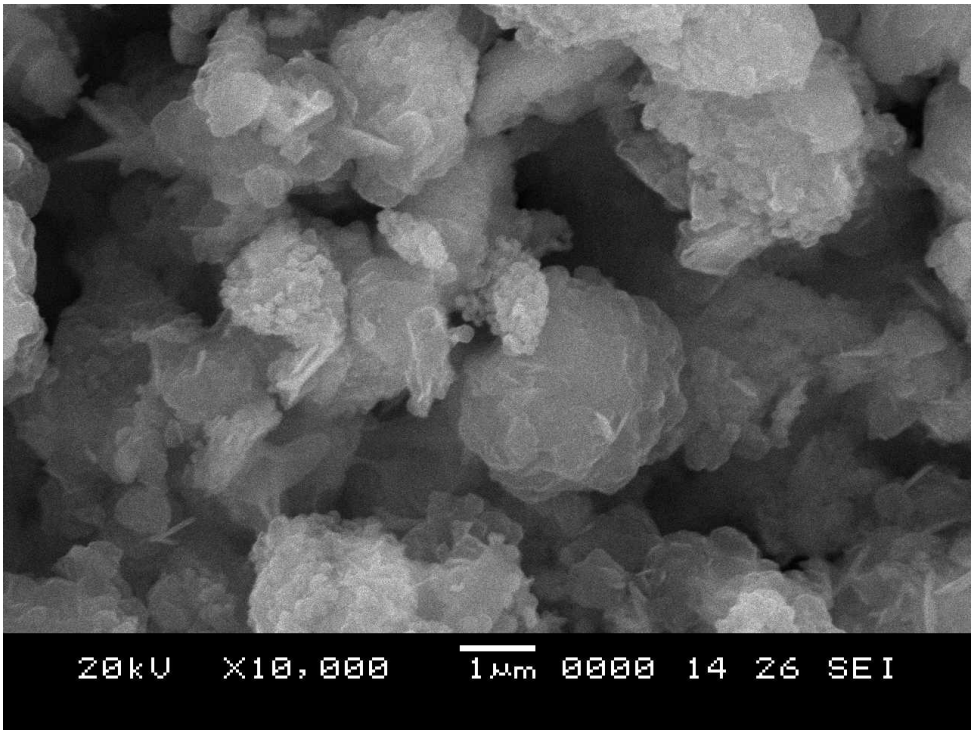

Figure 9. SEM of $ZnO_{0.7}$-Polyaniline $_{0.3}$ nanocomposites

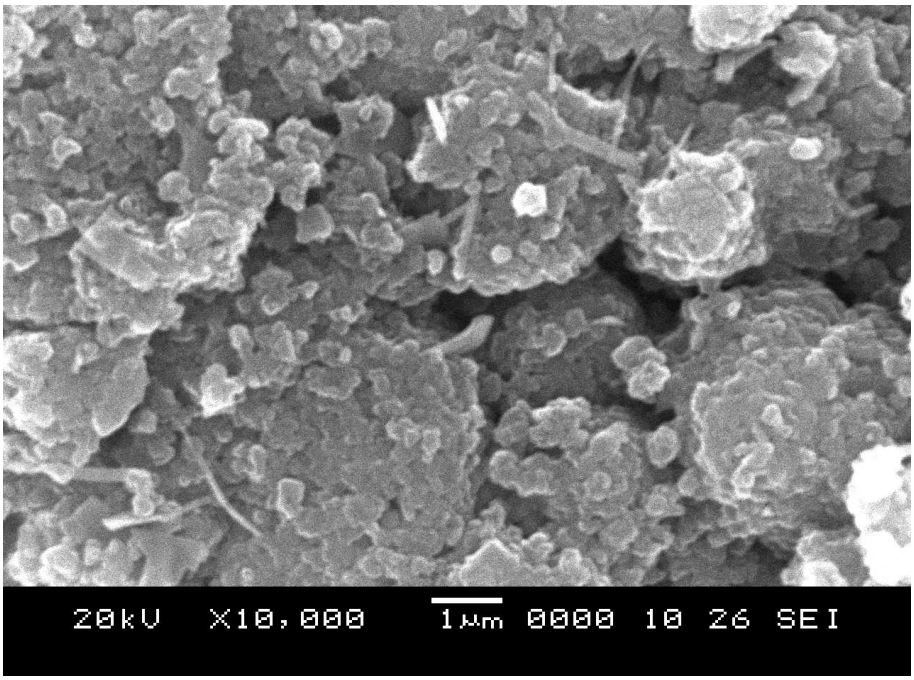

Figure 10. SEM of pure Polyaniline

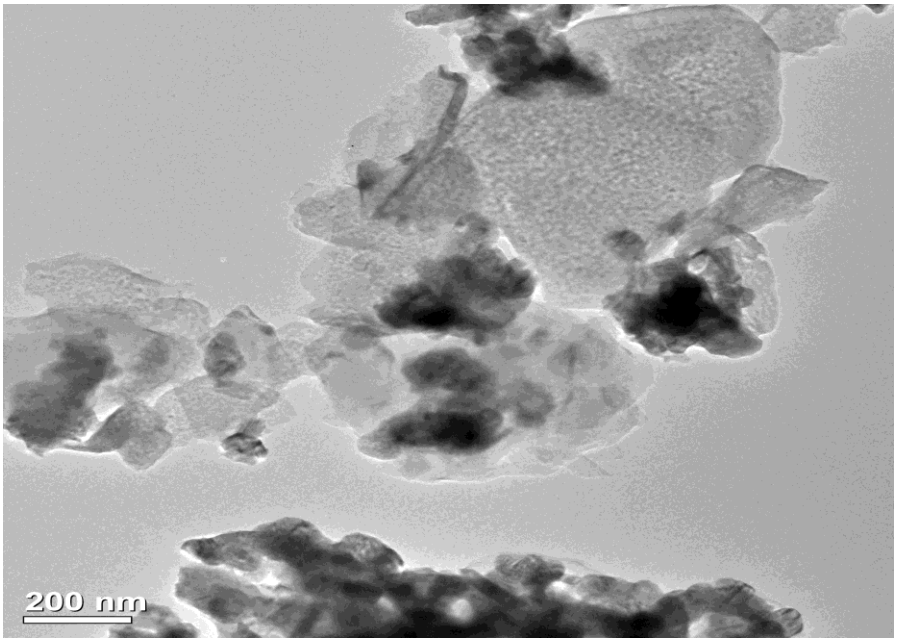

Figure 11. Transition electron microscope of ZnO-Polyanilinenanoparticles

Photo catalytic study of ZnO-Polyaniline nanocomposites

Under the UV light, the photodegradation efficiency was tested by using methyl orange at a specific concentration in an aqueous solution. Reliable measurements were made of the photocatalytic activity of ZnO-Polyaniline nanocomposites. The provided A.R grade methyl orange was utilized. Two components made up the photocatalytic reactor as follow: a 100 mL Pyrex glass bottle and a high-pressure

Hg lamp (125 W) with a maximum emission wavelength of roughly 365 nm that was placed similar to the Pyrex glass bottle. The top of Pyrex glass bottle was placed in front of the UV lamp at a distance of 10 cm, with a light output of roughly 40 W. Each experiment was conducted at room temperature. To make the reaction suspensions, 100 mL of methyl orange solutions were mixed with 75 mg of ZnO-polyaniline powder. To establish adsorption equilibrium prior to the UV-visible irradiation, the suspensions were ultrasonically sonicated for 30 min, followed by 30 min of magnetic stirring in the dark. The suspensions of methyl orange and photocatalyst were then continuously stirred while exposed to the UV-visible light. A Shimadzu (UV-160 PC Japan) UV-Visible spectrophotometer was used to measure the deterioration of methyl orange with time in the wavelength range of 250–600 nm. At varied reaction periods, the reaction suspensions were used as the source for analytical samples. Centrifuged at 8000 rpm for 15 min, and then analyzed. The UV-visible spectrophotometer was used to record the absorbance of the solutions in the 250–600 nm range to track the photodegradation efficiency. The absorbance readings of the original and analytical samples were used to calculate the decolorization effectiveness as a result of time. All of the photocatalytic tests employed nanocomposites made of ZnO and polyaniline.

It was investigated how organic dyes degraded catalytically at room temperature, under irradiation or darkness for predetermined periods of time. Through the UV-Vis spectroscopy, the dye concentrations in each sample were examined, and their absorptions at distinctive wavelengths were detected. By using calibration curves, the dye concentrations were determined. The decolonization efficiencies of the dyes are estimated by the following equation:

$$\text{Degradation (\%)} = Co - C/Co \times 100$$

Where Co represents the concentration of the dye before illumination, C denotes the concentration of dye after a certain irradiation time, correspondingly. After some repetitions, the best results were obtained in ZnO 0.7-Polyaniline 0.3 nanocomposites about 75 % degradation of methyl orange was observed under visible light within 140 minutes (Figure 12).

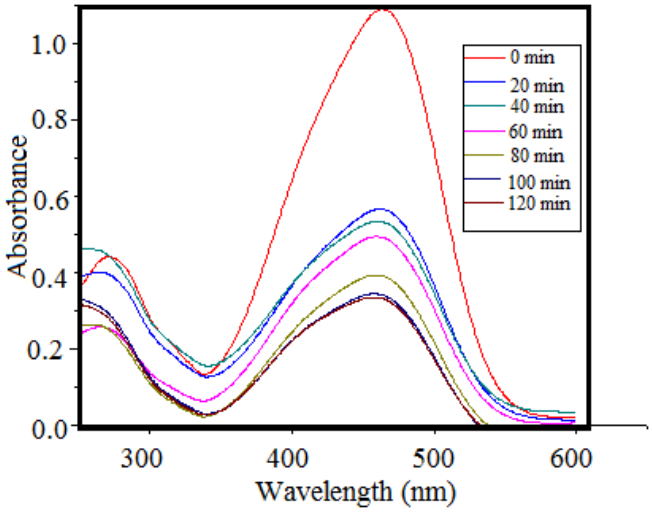

Figure 12. TheMO degradation graph under visible light by using ZnO 0.7 Polyaniline 0.3 nanocomposites

Conclusion

For the synthesis of photocatalytic ZnO-polyaniline nanocomposites, we have created a fresh, quick, and energy-efficient technique. Precipitation is a fairly straightforward process that may be readily expanded to make various oxide nanoparticles. By examining degradation efficiency, it was discovered that ZnO-Polyaniline generated by the precipitation technique plays a significant role in photocatalytic performance. The particle had a wurtzite structure and a spherical form. Crystallinity diminishes as the proportion of polyaniline in ZnO rises. The photocatalytic results revealed that increased polyaniline content of pure ZnO had an impact on how well ZnO nanoparticles degraded. Naturally, we discovered that adding more polyaniline to pure ZnO might boost the photodegradation efficiency. With ZnO 0.7 Polyanline, 0.3 composites and 0.75mg of catalyst were loaded, and the photocatalytic breakdown of methyl orange was mostly effective within 140 minutes. The MO degrading efficiency was higher than what was previously mentioned.

Orcid

Rajesh J. Kavade:
https://www.orcid.org/0000-0002-1418-9380
Renukacharya Ganpati Khanapure:
https://www.orcid.org/0000-0002-1418-9380

References

[1] S. Sarmah, A. Kumar, *Indian J. Phys.,* **2011**, *85*, 713–726. [Crossref], [Google Scholar], [Publisher]
[2] J. Mahmoud, O. Ghareeb, Y. Mahmood, *J. Med. Chem. Sci.*, 2022, 5, 76-81. [Crossref], [Google Scholar], [Publisher]
[3] V. Adams, J. Marley, *Br. Dent. J.*, **2007**, *203*, 585–591. [Crossref], [Google Scholar], [Publisher]
[4] A.J. Linz, R.K. Greenham, L.F. Fallon, *J. Occup. Environ. Med.,* **2006**, *48*, 523–530. [Crossref], [Google Scholar], [Publisher]
[5] D.P. Singh, *Sci. Adv. Mater.,* **2010**, *2*, 245–272. [Crossref], [Google Scholar], [Publisher]
[6] S.S. Ray, M. Biswas, *Synth. Met.,* **2000**, *108*, 231–236. [Crossref], [Google Scholar], [Publisher]
[7] S. Ameen, M.S. Akhtar, Y.S. Kim, O. Yang, H. Shin, *Colloid Polym. Sci.,* **2011**, *289*, 415–421. [Crossref], [Google Scholar], [Publisher]
[8] R. Saravanan, H. Shankar, T. Prakash, V. Narayanan, A. Stephen, *Mater. Chem.Phys.,* **2011**, *125*, 277–280. [Crossref], [Google Scholar], [Publisher]
[9] K. Gupta, P.C. Jana, A.K. Meikap, *J. Appl. Phys.*, **2011**, *109*, 123713/1-123713/9. [Google Scholar], [Publisher]
[10] S. Ameen, M.S. Akhtar, S.G. Ansari, O. Yang, H. Shin, *Super lattices Micro struct.,* **2009**, *46*, 872–880. [Crossref], [Google Scholar], [Publisher]
[11] B.K. Sharma, A.K. Gupta, N. Khare, S.K. Dhaan, H.C. Gupta, *Synth. Met.,* **2009**, *159*, 391–395. [Crossref], [Google Scholar], [Publisher]
[12] M. Shaolin, K. Jinqing, *Synth. Met.*, **2002**, *132*, 29–33. [Crossref], [Google Scholar], [Publisher]
[13] Z. Mandic, L. Duic, *J. Electroanal. Chem.,* **1996**, *403*, 133–141. [Crossref], [Google Scholar], [Publisher]
[14] S. Ferrere, A. Zaban, B.A. Gregg, *J. Phys. Chem. B*, **1997**, *101*, 4490–4493. [Crossref], [Google Scholar], [Publisher]
[15] S.E. Shaheen, C.J. Brabec, F. Padinger, T. Fromherz, J.C. Hummelen, N.S. Sarıciftc, *Appl. Phys. Lett.*, **2001**, *78*, 841–843. [Crossref], [Google Scholar], [Publisher]
[16] Z.M. Mbhele, M.G. Sakmane, C.G.C.E. van Sittert, J.M. Nedeljkovic, V. Djokovic,A.S. Luyt, *Chem. Mater.,* **2003**, *15*, 5019–5024. [Crossref], [Google Scholar], [Publisher]

[17] M.R. Karim, C.J. Lee, Y.T. Park, M.S. Lee, *J. Polym. Chem.,* **2006**, *14*, 5283–5290. [Crossref], [Google Scholar], [Publisher]
[18] Z. Zhang, M. Han, *J. Mater. Chem.*, **2003**, *13*, 641–643. [Crossref], [Google Scholar], [Publisher]
[19] P.K. Khanna, S. Lonker, V.S. Subbarao, K.W. Jun, *Mater. Chem. Phys.,***2004**, *87*, 49–52. [Crossref], [Google Scholar], [Publisher]
[20] U. Ozgur, Y.I. Alivov, C. Liu, A. Teke, M.A. Reshchikov, S. Do˘gan, V. Avrutin, S.-J.Cho, H. Morkoc, *J. Appl. Phys.*, **2005**, 98. [Crossref], [Google Scholar], [Publisher]
[21] H.S. Bae, M.H. Yoon, J.H. Kim, S. Im, *Appl. Phys. Lett.*, **2003**, *83*, 5313–5315. [Crossref], [Google Scholar], [Publisher]
[22] F.C.M. Van de pol, *Ceram. Bull.*, **1990**, 69, 1959–1965. [Google Scholar], [Publisher]
[23] Z.C. Jin, I. Hamberg, C.G. Granqvist, B.E. Sernelius, K.F. Berggren, *Thin Solid Films,* **1988**, *164*, 381–386. [Crossref], [Google Scholar], [Publisher]
[24] L. Spanhel, M.A. Anderson, *J. Am. Chem. Soc.,* **1991**, *113*, 2826–2833.[Crossref], [Google Scholar], [Publisher]
[25] B.S. Hote, T.A. J. Siddiqui, P.M. Pisal, V.S. More,*Polycyclic Aromatic Compounds.,* **2021**, 1-9. [Crossref], [Google Scholar], [Publisher]
[26] G. Gustafsson, Y. Cao, G.M. Treacy, F. Klavetter, N. Colaneri, A. Heeger, *Nature.,* **1992**, *357*, 477–479. [Crossref], [Google Scholar], [Publisher]
[27] M.J. Sailor, E.J. Ginsburg, C.B. Gorman, A. Kumar, R.H. Grubbs, N.S. Lewis, *Science*, **1990**, *249*, 1146–1149. [Crossref], [Google Scholar], [Publisher]
[28] H.Salavati, A.Teimouri, S. Kazemi, *Chemical Methodologies*, **2017**, *1*(1), 12-27. [Crossref], [Google Scholar], [Publisher]
[29] R.G. Khanapure, S.K.Awate, S.V.Patil, *Asian Journal of Chemistry*, **2021**, *33*(8), 1805-1810. [Crossref], [Google Scholar], [Publisher]
[30] R.G. Khanapure, A.A.Ghanwat, S.K. Awate, U.S.Gawali, R.J. Kavade, P.H. Salunkhe, S.V. Patil, *Polymer Bulletin,* **2022**, 1-13. [Crossref], [Google Scholar], [Publisher]
[31] R. Gangopadhyay, A. De, *Chem. Mater.,* **2000**, *12*, 608–622. [Crossref], [Google Scholar], [Publisher]
[32] M. Zhang, S.L. Fang, A.A. Zakhidov, S.B. Lee, A.E. Aliev, C.D. Williams, K.R. Atkinson,R.H. Baughman, *Science,* **2005**, *309*, 1215–1219. [Crossref], [Google Scholar], [Publisher]
[33] K. Lee, Z. Wu, Z. Chen, F. Ren, S.J. Pearton, A.G. Rinzler, *Nano Lett.,* **2004,** *4*, 911–914. [Crossref], [Google Scholar], [Publisher]
[34] M. Chang, X.L. Cao, H. Zheng, L. Zhang, *Chem. Phys. Lett.*, **2007**, *446*, 370–373. [Crossref], [Google Scholar], [Publisher]
[35] J.P. Pouget, C.H. Hsu, A.G. MacDiarmid, A.J. Epstein, *Synth. Met.,* **1995**, *69*, 119–120. [Crossref], [Google Scholar], [Publisher]